VII International Conference on Computational Methods for Coupled Problems in Science and Engineering
COUPLED PROBLEMS 2017
M. Papadrakakis, E. Oñate and B. Schrefler (Eds)

NUMERICAL STABILITY OF EXPLICIT AND IMPLICIT CO-SIMULATION METHODS

P. LI*, T. MEYER*, D. LU* AND B. SCHWEIZER*

*Institute of Applied Dynamics
Technical University of Darmstadt
Otto-Berndt-Strasse 2, 64287 Darmstadt, Germany
e-mail: {li, meyer, lu, schweizer}@ad.tu-darmstadt.de, www.ad.tu-darmstadt.de

Key words: Co-Simulation, Numerical Stability, Implicit, Explicit, Applied-Force Coupling

Abstract. Within a co-simulation approach, the subsystems are integrated by specific solvers; data exchange is accomplished only at certain user-defined macro-time points. Due to the approximation of the coupling variables by polynomials and as a result of the data exchange between the subsystems, errors are introduced, which may entail severe stability problems. Hence, the development of stabilized coupling techniques is of special interest. To analyze the stability of co-simulation approaches, we consider two coupled Dahlquist's equations so that the conventional linear stability analysis can be applied. Consequently, the stability of the co-simulation method can be determined by calculating the spectral radius of the governing system of recurrence equations. The numerical stability of classical explicit and implicit co-simulation techniques is investigated here. Also, modified coupling approaches are discussed, which show an improved stability behavior.

1 INTRODUCTION

To couple two or more solvers in time domain, co-simulation methods can be used advantageously in order to analyze multidisciplinary systems, e.g. for investigating flexible multibody systems [1] or for studying Fluid-Structure-Interaction (FSI) problems [2]. Especially for examining vehicle systems, co-simulation has found increasing usage in the last decades [3]. For analyzing monodisciplinary problems, one may also apply co-simulation approaches in order to speed up the simulation by parallelizing the overall dynamical system. For instance, "subcycling algorithms", which are widely applied in the framework of structural dynamics [4], can be regarded as explicit co-simulation methods.

Making use of co-simulation algorithms, subsystems are integrated with individual, specific solvers and coupling data are exchanged at certain discretized time points (macro-time points) only. Usually, the coupling variables are unknown in the integrating process and have therefore to be approximated using polynomials, for instance. As a result, numerical errors are introduced which may result in instability problems.

In this paper, the stability analysis is accomplished with the help of two coupled Dahlquist's equations. A system of two mass-oscillators, connected by a spring-damper element, is used in Section 2 in order to derive the linear system of recurrence equations, which is applied to

analyze the numerical stability of a coupling approach. In Section 3, different explicit and implicit co-simulation algorithms will be considered and corresponding stability plots will be presented in Section 4. A summary of the results is given in Section 5.

2 TEST MODEL FOR STABILITY ANALYSIS OF CO-SIMULATION METHODS

The numerical stability of time integration schemes is defined by Dahlquist's test equation. From the mechanical point of view, this equation can be interpreted as the complex representation of the equations of motion of the autonomous linear mass-spring-damper oscillator. To analyze the numerical stability of co-simulation methods, it is therefore straightforward to use the linear two-mass oscillator as test model, see Figure 1.

Dahlquist's test equation is given by

$$\dot{y}(t) = \Lambda \cdot y(t) \tag{1}$$

where $y(t)$ is a scalar function of time and Λ an arbitrary complex constant. The 2-DOF oscillator can be regarded as two single-mass oscillators (masses m_1/m_2, spring constant c_1/c_2, damping coefficients d_1/d_2), which are coupled by the coupling spring c_c and the coupling damper d_c. Hence, the two-mass oscillator can be considered as two Dahlquist's equations, which are coupled by a linear constitutive equation.

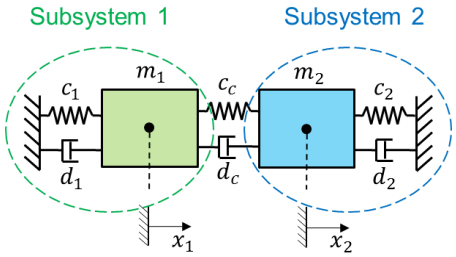

Figure 1: Test model for analyzing the stability of co-simulation methods: linear two-mass oscillator

The equations of motion for the coupled oscillator read as

$$\begin{aligned}
\dot{x}_1 &= v_1 \\
\dot{v}_1 &= -\frac{c_1}{m_1}x_1 - \frac{d_1}{m_1}v_1 + \frac{c_c}{m_1}\cdot(x_2 - x_1) + \frac{d_c}{m_1}\cdot(v_2 - v_1) \\
\dot{x}_2 &= v_2 \\
\dot{v}_2 &= -\frac{c_2}{m_2}x_2 - \frac{d_2}{m_2}v_2 - \frac{c_c}{m_2}\cdot(x_2 - x_1) - \frac{d_c}{m_2}\cdot(v_2 - v_1).
\end{aligned} \tag{2}$$

For the stability analysis of co-simulation methods, it is useful to introduce dimensionless variables. We assume that $\bar{x}_1, \bar{x}_2$ are properly chosen dimensionless position coordinates. The variables $\bar{v}_1 = H \cdot d\bar{x}_1/dt$ and $\bar{v}_2 = H \cdot d\bar{x}_2/dt$ denote dimensionless velocities, where H denotes the macro-step size of the co-simulation approach. The dimensionless time is defined by $\bar{t} = t/H$. Furthermore, it is suitable to define the following 7 parameters:

$$\begin{gathered}
\bar{c}_1 = \frac{c_1 \cdot H^2}{m_1}, \quad \bar{d}_1 = \frac{d_1 \cdot H}{m_1}, \quad \alpha_{m21} = \frac{m_2}{m_1}, \quad \alpha_{c21} = \frac{c_2}{c_1}, \quad \alpha_{d21} = \frac{d_2}{d_1}, \\
\alpha_{cc1} = \frac{c_c}{c_1}, \quad \alpha_{dc1} = \frac{d_c}{d_1}.
\end{gathered} \tag{3}$$

The dimensionless equations of motion for the coupled oscillator can be written as

$$\begin{aligned}
\bar{x}_1' &= \bar{v}_1 \\
\bar{v}_1' &= -\bar{c}_1 \cdot \bar{x}_1 - \bar{d}_1 \cdot \bar{v}_1 + \alpha_{cc1} \cdot \bar{c}_1 \cdot (\bar{x}_2 - \bar{x}_1) + \alpha_{dc1} \cdot \bar{d}_1 \cdot (\bar{v}_2 - \bar{v}_1) \\
\bar{x}_2' &= \bar{v}_2 \\
\bar{v}_2' &= -\frac{\alpha_{c21}}{\alpha_{m21}} \cdot \bar{c}_1 \cdot \bar{x}_2 - \frac{\alpha_{d21}}{\alpha_{m21}} \cdot \bar{d}_1 \cdot \bar{v}_2 - \frac{\alpha_{cc1}}{\alpha_{m21}} \cdot \bar{c}_1 \cdot (\bar{x}_2 - \bar{x}_1) - \frac{\alpha_{dc1}}{\alpha_{m21}} \cdot \bar{d}_1 \cdot (\bar{v}_2 - \bar{v}_1) \ .
\end{aligned} \tag{4}$$

In compact form, the above system of equations can be written as

$$\boldsymbol{z}' = \boldsymbol{A} \cdot \boldsymbol{z} \qquad \text{with } \boldsymbol{z} = (\bar{x}_1 \quad \bar{v}_1 \quad \bar{x}_2 \quad \bar{v}_2)^T \in \mathbb{R}^4 \text{ and}$$

$$\boldsymbol{A} = \begin{pmatrix} 0 & 1 & 0 & 0 \\ -(1+\alpha_{cc1}) \cdot \bar{c}_1 & -(1+\alpha_{dc1}) \cdot \bar{d}_1 & \alpha_{cc1} \cdot \bar{c}_1 & \alpha_{dc1} \cdot \bar{d}_1 \\ 0 & 0 & 0 & 1 \\ \frac{\alpha_{cc1}}{\alpha_{m21}} \cdot \bar{c}_1 & \frac{\alpha_{dc1}}{\alpha_{m21}} \cdot \bar{d}_1 & -\frac{\alpha_{c21}+\alpha_{cc1}}{\alpha_{m21}} \cdot \bar{c}_1 & -\frac{\alpha_{d21}+\alpha_{dc1}}{\alpha_{m21}} \cdot \bar{d}_1 \end{pmatrix} \in \mathbb{R}^{4\times 4} . \tag{5}$$

Obviously, the two-mass oscillator is a mechanically stable system, if $m_1, m_2, c_1, c_2, d_1, d_2 > 0$.

Regarding the two-mass oscillator as two coupled single-mass oscillators, the equations of motion can be formulated in a modular manner according to

$$\begin{aligned}
\boldsymbol{z}' &= \boldsymbol{A} \cdot \boldsymbol{z} + \boldsymbol{B} \cdot \boldsymbol{u} \\
\boldsymbol{g} &= \boldsymbol{C} \cdot \boldsymbol{z} + \boldsymbol{D} \cdot \boldsymbol{u} = \boldsymbol{0} \ .
\end{aligned} \tag{6}$$

The vector $\boldsymbol{z} = (\bar{x}_1 \quad \bar{v}_1 \quad \bar{x}_2 \quad \bar{v}_2)^T \in \mathbb{R}^4$ collects the dimensionless state variables, while the vector $\boldsymbol{u} = (\tilde{\bar{x}}_1 \quad \tilde{\bar{v}}_1 \quad \tilde{\bar{x}}_2 \quad \tilde{\bar{v}}_2 \quad \bar{\lambda}_c)^T \in \mathbb{R}^5$ contains the coupling variables required for the three different test models considered here, namely the force/force-, the force/displacement- and the displacement/displacement-decomposition test model. $\bar{\lambda}_c = \lambda_c \cdot H^2/m_1$ terms the dimensionless coupling force, which is a function of the state variables of the subsystems. $\boldsymbol{A}, \boldsymbol{B}, \boldsymbol{C}$ and $\boldsymbol{D}$ are corresponding coefficient matrices (vectors).

In the framework of a force/force-coupling approach [5], the basic idea is to divide the two-mass oscillator into two single-mass oscillators (two subsystems), which are driven by the coupling force λ_c, see Figure 2.

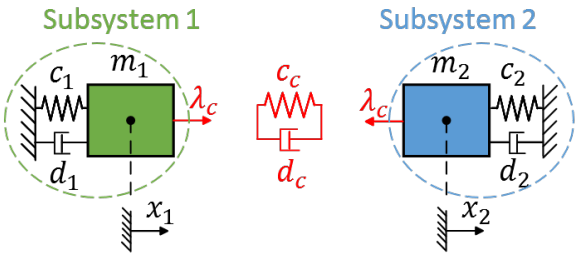

Figure 2: Co-simulation test model for force/force-coupling approach

Regarding the general Eq. (6), it is straightforward to derive the governing system matrices for the force/force-coupling approach, which read as

$$\boldsymbol{A}_{FF} = \begin{pmatrix} 0 & 1 & 0 & 0 \\ -\bar{c}_1 & -\bar{d}_1 & 0 & 0 \\ 0 & 0 & 0 & 1 \\ 0 & 0 & -\frac{\alpha_{c21}}{\alpha_{m21}} \cdot \bar{c}_1 & -\frac{\alpha_{d21}}{\alpha_{m21}} \cdot \bar{d}_1 \end{pmatrix}, \quad \boldsymbol{B}_{FF} = \begin{pmatrix} 0 & 0 & 0 & 0 & 0 \\ 0 & 0 & 0 & 0 & 1 \\ 0 & 0 & 0 & 0 & 0 \\ 0 & 0 & 0 & 0 & -\frac{1}{\alpha_{m21}} \end{pmatrix}, \tag{7}$$

$$\boldsymbol{C}_{FF} = (\alpha_{cc1} \cdot \bar{c}_1 \quad \alpha_{dc1} \cdot \bar{d}_1 \quad -\alpha_{cc1} \cdot \bar{c}_1 \quad -\alpha_{dc1} \cdot \bar{d}_1), \quad \boldsymbol{D}_{FF} = (0 \quad 0 \quad 0 \quad 0 \quad 1).$$

For the case that the co-simulation test model is decomposed by a force/displacement-coupling approach, subsystem 1 will be a force-driven and subsystem 2 a base-point excited single-mass oscillator as illustrated in Figure 3.

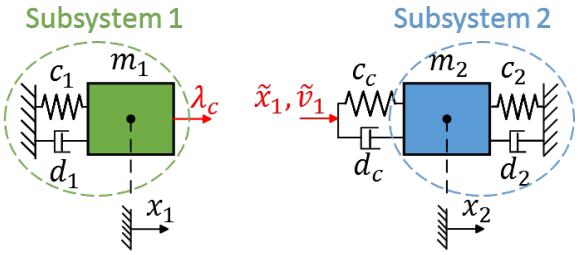

Figure 3: Co-simulation test model for force/displacement-coupling approach

Applying a force/displacement-decomposition, the coupling force λ_c is replaced in subsystem 2 with the help of state variables of subsystem 1, which fulfill the coupling condition $g_c := \lambda_c - c_c \cdot (x_2 - x_1) - d_c \cdot (v_2 - v_1) = 0$. Due to the fact that the state variables x_1 and v_1 are unknown in subsystem 2, they are replaced by two additional coupling variables, which are denoted by $\tilde{x}_1$ and $\tilde{v}_1$.Therefore, the decomposed subsystems can be described by Eq. (6) with the following dimensionless coefficient matrices

$$\boldsymbol{A}_{FD} = \begin{pmatrix} 0 & 1 & 0 & 0 \\ -\bar{c}_1 & -\bar{d}_1 & 0 & 0 \\ 0 & 0 & 0 & 1 \\ 0 & 0 & -\frac{\alpha_{c21} + \alpha_{cc1}}{\alpha_{m21}} \cdot \bar{c}_1 & -\frac{\alpha_{d21} + \alpha_{dc1}}{\alpha_{m21}} \cdot \bar{d}_1 \end{pmatrix},$$

$$\boldsymbol{B}_{FD} = \begin{pmatrix} 0 & 0 & 0 & 0 & 0 \\ 0 & 0 & 0 & 0 & 1 \\ 0 & 0 & 0 & 0 & 0 \\ \frac{\alpha_{cc1}}{\alpha_{m21}} \cdot \bar{c}_1 & \frac{\alpha_{dc1}}{\alpha_{m21}} \cdot \bar{d}_1 & 0 & 0 & 0 \end{pmatrix}, \tag{8}$$

$$\boldsymbol{C}_{FD} = \begin{pmatrix} \alpha_{cc1} \cdot \bar{c}_1 & \alpha_{dc1} \cdot \bar{d}_1 & -\alpha_{cc1} \cdot \bar{c}_1 & -\alpha_{dc1} \cdot \bar{d}_1 \\ -1 & 0 & 0 & 0 \\ 0 & -1 & 0 & 0 \end{pmatrix}, \quad \boldsymbol{D}_{FD} = \begin{pmatrix} 0 & 0 & 0 & 0 & 1 \\ 1 & 0 & 0 & 0 & 0 \\ 0 & 1 & 0 & 0 & 0 \end{pmatrix}.$$

When a displacement/displacement-coupling approach is used to decompose the two-mass oscillator, each subsystem is described by a base-point excited single-mass oscillator, see Figure 4.

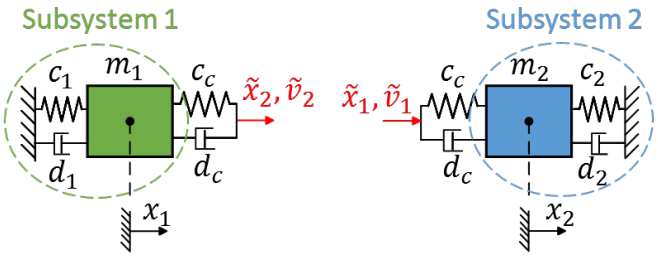

Figure 4: Co-simulation test model for displacement/displacement-coupling approach

For this purpose, the coupling spring/damper system has to be duplicated, i.e. the coupling variable λ_c is replaced in both subsystems by introducing the four coupling variables $\tilde{x}_1, \tilde{x}_2$ and $\tilde{v}_1, \tilde{v}_2$. The corresponding coefficient matrices characterizing the decomposed system are given by

$$\boldsymbol{A}_{DD} = \begin{pmatrix} 0 & 1 & 0 & 0 \\ -(1+\alpha_{cc1})\bar{c}_1 & -(1+\alpha_{dc1})\bar{d}_1 & 0 & 0 \\ 0 & 0 & 0 & 1 \\ 0 & 0 & -\dfrac{\alpha_{c21}+\alpha_{cc1}}{\alpha_{m21}}\bar{c}_1 & -\dfrac{\alpha_{d21}+\alpha_{dc1}}{\alpha_{m21}}\bar{d}_1 \end{pmatrix},$$

$$\boldsymbol{B}_{DD} = \begin{pmatrix} 0 & 0 & 0 & 0 & 0 \\ 0 & 0 & \alpha_{cc1}\cdot\bar{c}_1 & \alpha_{dc1}\cdot\bar{d}_1 & 0 \\ 0 & 0 & 0 & 0 & 0 \\ \dfrac{\alpha_{cc1}}{\alpha_{m21}}\cdot\bar{c}_1 & \dfrac{\alpha_{dc1}}{\alpha_{m21}}\cdot\bar{d}_1 & 0 & 0 & 0 \end{pmatrix}, \tag{9}$$

$$\boldsymbol{C}_{DD} = \begin{pmatrix} -1 & 0 & 0 & 0 \\ 0 & -1 & 0 & 0 \\ 0 & 0 & -1 & 0 \\ 0 & 0 & 0 & -1 \end{pmatrix}, \quad \boldsymbol{D}_{DD} = \begin{pmatrix} 1 & 0 & 0 & 0 & 0 \\ 0 & 1 & 0 & 0 & 0 \\ 0 & 0 & 1 & 0 & 0 \\ 0 & 0 & 0 & 1 & 0 \end{pmatrix}.$$

3 DIRECT AND EXTENDED CO-SIMULATION ALGORITHMS

3.1 Explicit and implicit direct co-simulation algorithm

The direct implicit co-simulation methods investigated here are based on a predictor/corrector approach, which is performed in three steps. To illustrate the integration process, it is convenient to define the vectors $\boldsymbol{z}_{N+1}, \boldsymbol{z}_N$, etc., which collect the state variables of the two subsystems at the macro-time points $\bar{T}_{N+1}, \bar{T}_N$, etc.. The initial conditions for the macro-time step from $\bar{T}_N$ to $\bar{T}_{N+1}$ are given by the state vector $\boldsymbol{z}_N$ at the time point $\bar{T}_N$. The upper indices p and $*$ (e.g. $\boldsymbol{z}_{N+1}^{p}$ and $\boldsymbol{z}_{N+1}^{*}$) term predicted and arbitrary state variables, whereas the corrected variables (e.g. $\boldsymbol{z}_{N+1}$) are defined without an upper index. In the following analysis, only the case of quadratic approximation polynomials ($k = 2$) in combination with force/force-decomposition is discussed in order to derive the governing system of recurrence equations for the decomposed two-mass oscillator system.

Step 1: Predictor step

An analytical integration of subsystem 1 and subsystem 2 with the predicted (extrapolated)

coupling force $\bar{\lambda}_c^p(\bar{t}) = P_{\bar{\lambda}_c}^p\left[\left(\bar{T}_N, \bar{\lambda}_{c,N}\right), \left(\bar{T}_{N-1}, \bar{\lambda}_{c,N-1}\right), \left(\bar{T}_{N-2}, \bar{\lambda}_{c,N-2}\right); \bar{t}\right]$ yields the predicted state variables at the macro-time point $\bar{T}_{N+1}$

$$\boldsymbol{z}_{N+1}^p = \boldsymbol{z}_{N+1}^p\left(\bar{\lambda}_{c,N}, \bar{\lambda}_{c,N-1}, \bar{\lambda}_{c,N-2}, \boldsymbol{z}_N\right). \tag{10}$$

Step 2: Calculation of corrected coupling variables

By analytically integrating both subsystems from $\bar{T}_N$ to $\bar{T}_{N+1}$ with initial conditions $\boldsymbol{z}_N$ and the interpolated coupling force $\bar{\lambda}_c^*(\bar{t}) = P_{\bar{\lambda}_c}^*\left[\left(\bar{T}_{N+1}, \bar{\lambda}_{c,N+1}^*\right), \left(\bar{T}_N, \bar{\lambda}_{c,N}\right), \left(\bar{T}_{N-1}, \bar{\lambda}_{c,N-1}\right); \bar{t}\right]$, we get the following state variables at the macro-time point $\bar{T}_{N+1}$

$$\boldsymbol{z}_{N+1}^* = \boldsymbol{z}_{N+1}^*\left(\bar{\lambda}_{c,N+1}^*, \bar{\lambda}_{c,N}, \bar{\lambda}_{c,N-1}, \boldsymbol{z}_N\right). \tag{11}$$

Note that $\bar{\lambda}_{c,N+1}^*$ represents an arbitrary coupling force at the macro-time point $\bar{T}_{N+1}$.
Rewriting the coupling condition with the arbitrary state variables $\boldsymbol{z}_{N+1}^*$ yields

$$\bar{g}_{c\lambda,N+1} \coloneqq \bar{\lambda}_{c,N+1}^* - \alpha_{cc1} \cdot \bar{c}_1 \cdot \left(\bar{x}_{2,N+1}^* - \bar{x}_{1,N+1}^*\right) - \alpha_{dc1} \cdot \bar{d}_1 \cdot \left(\bar{v}_{2,N+1}^* - \bar{v}_{1,N+1}^*\right). \tag{12}$$

Furthermore, the Jacobian matrix of the coupling equation $\bar{g}_{c\lambda,N+1}$ with respect to the coupling force, i.e. $J_c = \frac{\partial \bar{g}_{c\lambda,N+1}}{\partial \bar{\lambda}_{c,N+1}^*}$, can be calculated. Since only one coupling variable $\bar{\lambda}_{c,N+1}$ is needed for the force/force-coupling method, the Jacobian matrix is represented by a scalar value. As a result, we obtain the linearized coupling equation as

$$\bar{g}_{c\lambda,linear} \coloneqq \bar{g}_{c\lambda,N+1}^p + J_c \cdot \left(\bar{\lambda}_{c,N+1} - \bar{\lambda}_{c,N+1}^p\right) = 0. \tag{13}$$

Solving Eq. (13) gives the corrected coupling force $\bar{\lambda}_{c,N+1}$.

Step 3: Corrector step

Using the corrected (interpolated) polynomial with the corrected coupling force $\bar{\lambda}_{c,N+1}$ from Eq. (13), an analytical integration of subsystem 1 and subsystem 2 gives the corrected states

$$\boldsymbol{z}_{N+1} = \boldsymbol{z}_{N+1}\left(\bar{\lambda}_{c,N+1}, \bar{\lambda}_{c,N}, \bar{\lambda}_{c,N-1}, \boldsymbol{z}_N\right). \tag{14}$$

Substituting the coupling forces at the time points $\bar{T}_{N+1}, \bar{T}_N$ and $\bar{T}_{N-1}$with the help of the coupling equations results in a relationship of the form

$$\boldsymbol{A}_{N+1} \cdot \boldsymbol{z}_{N+1} + \boldsymbol{A}_N \cdot \boldsymbol{z}_N + \boldsymbol{A}_{N-1} \cdot \boldsymbol{z}_{N-1} = \boldsymbol{0}. \tag{15}$$

The real-valued matrices $\boldsymbol{A}_{N+1}, \boldsymbol{A}_N$ and $\boldsymbol{A}_{N-1} \in \mathbb{R}^{4\times4}$ are constant and depend only on the seven parameters of the co-simulation test model defined above. The linear recurrence system (15) can simply be solved by the exponential approach $\boldsymbol{z}_N = \hat{\boldsymbol{z}} \cdot \Lambda^N$, where Λ denotes the eigenvalue and $\hat{\boldsymbol{z}}$ the Eigenvector of the system. Therefore, the corresponding co-simulation method is called numerical stable, if the spectral radius of the recurrence system is smaller than 1.
In the framework of an explicit co-simulation approach, we consider only step 1, i.e. both subsystems are integrated with the help of extrapolation polynomials. Substituting the coupling forces with the help of the coupling conditions, we get a recurrence system of the form

$$\boldsymbol{A}_{N+1} \cdot \boldsymbol{z}_{N+1} + \boldsymbol{A}_N \cdot \boldsymbol{z}_N + \boldsymbol{A}_{N-1} \cdot \boldsymbol{z}_{N-1} + \boldsymbol{A}_{N-2} \cdot \boldsymbol{z}_{N-2} = \boldsymbol{0}. \tag{16}$$

3.2 Extended implicit co-simulation algorithm

The key concept for the extended co-simulation approaches is to extend the coupling equations by derivatives (D-Extension) and integrals (I-Extension) of the original constitutive equations [6]. Therefore, the coupling variables have to be discretized not only at the macro-time points $\bar{T}_{N+1}, \bar{T}_{N+2}$, etc., but also at intermediate time points, e.g. $\bar{T}_{N+1/2}, \bar{T}_{N+3/2}$, etc.. Corresponding polynomials for approximation order $k = 0, 1, 2$ are shown in Figure 5.

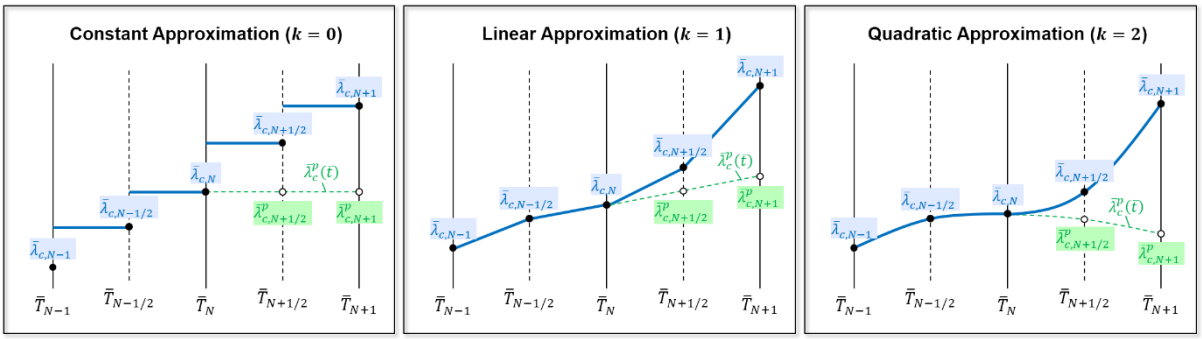

Figure 5: Extended extrapolation and interpolation polynomials for constant, linear and quadratic approximation

Note that the sampling time points between macro steps can be arbitrary and may have an influence on the stability behavior. Here, we consider only the case of equidistantly distributed time points ($\bar{T}_{N+1/2}, \bar{T}_{N+3/2}$, etc.). Based on a predictor-corrector approach, the three integration steps explained above have to be performed with the extended polynomials. In the following, sub-indices D and I (e.g. $\boldsymbol{z}^p_{N+1,D}, \boldsymbol{z}^p_{N+1,I}$) are used to distinguish between D-Extension and I-Extension approaches.

Step 1: Predictor step

An analytical integration of subsystem 1 and subsystem 2 with predicted (extrapolated) coupling forces yields the predicted state variables at the macro-time point $\bar{T}_{N+1}$

$$\begin{aligned} \boldsymbol{z}^p_{N+1} &= \boldsymbol{z}^p_{N+1}(\bar{\lambda}_{c,N}, \bar{\lambda}_{c,N-1/2}, \bar{\lambda}_{c,N-1}, \boldsymbol{z}_N), \\ \boldsymbol{z}^p_{N+1,D} &= (\boldsymbol{z}^p_{N+1})' = \boldsymbol{z}^p_{N+1,D}(\bar{\lambda}_{c,N}, \bar{\lambda}_{c,N-1/2}, \bar{\lambda}_{c,N-1}, \boldsymbol{z}_N), \\ \boldsymbol{z}^p_{N+1,I} &= \int \boldsymbol{z}^p_{N+1}\, d\bar{t} = \boldsymbol{z}^p_{N+1,I}(\bar{\lambda}_{c,N}, \bar{\lambda}_{c,N-1/2}, \bar{\lambda}_{c,N-1}, \boldsymbol{z}_N). \end{aligned} \tag{17}$$

Step 2: Calculation of corrected coupling variables

By analytically integrating both subsystems from $\bar{T}_N$ to $\bar{T}_{N+1}$ and using interpolated coupling forces, we get the following state variables at the macro-time point $\bar{T}_{N+1}$

$$\begin{aligned} \boldsymbol{z}^*_{N+1} &= \boldsymbol{z}^*_{N+1}(\bar{\lambda}^*_{c,N+1}, \bar{\lambda}^*_{c,N+1/2}, \bar{\lambda}_{c,N}, \boldsymbol{z}_N), \\ \boldsymbol{z}^*_{N+1,D} &= (\boldsymbol{z}^*_{N+1})' = \boldsymbol{z}^*_{N+1,D}(\bar{\lambda}^*_{c,N+1}, \bar{\lambda}^*_{c,N+1/2}, \bar{\lambda}_{c,N}, \boldsymbol{z}_N), \\ \boldsymbol{z}^*_{N+1,I} &= \int \boldsymbol{z}^*_{N+1}\, d\bar{t} = \boldsymbol{z}^*_{N+1,I}(\bar{\lambda}^*_{c,N+1}, \bar{\lambda}^*_{c,N+1/2}, \bar{\lambda}_{c,N}, \boldsymbol{z}_N). \end{aligned} \tag{18}$$

Regarding the coupling conditions at the macro-time point $\bar{T}_{N+1}$, we have

$$\begin{aligned}
\bar{g}_{c\lambda} &:= \bar{\lambda}^*_{c,N+1} - \alpha_{cc1} \cdot \bar{c}_1 \cdot \left(\bar{x}^*_{2,N+1} - \bar{x}^*_{1,N+1}\right) - \alpha_{dc1} \cdot \bar{d}_1 \cdot \left(\bar{v}^*_{2,N+1} - \bar{v}^*_{1,N+1}\right), \\
\bar{g}_{c\lambda,D} &:= \bar{\lambda}^{*\prime}_{c,N+1} - \alpha_{cc1} \cdot \bar{c}_1 \cdot \left(\bar{v}^*_{2,N+1} - \bar{v}^*_{1,N+1}\right) - \alpha_{dc1} \cdot \bar{d}_1 \cdot \left(\bar{v}^{*\prime}_{2,N+1} - \bar{v}^{*\prime}_{1,N+1}\right), \\
\bar{g}_{c\lambda,I} &:= \int \left[\bar{\lambda}^*_{c,N+1} - \alpha_{cc1} \cdot \bar{c}_1 \cdot \left(\bar{x}^*_{2,N+1} - \bar{x}^*_{1,N+1}\right) - \alpha_{dc1} \cdot \bar{d}_1 \cdot \left(\bar{v}^*_{2,N+1} - \bar{v}^*_{1,N+1}\right)\right] d\bar{t}.
\end{aligned} \tag{19}$$

Within this step, we have to derive the Jacobian matrix of the coupling equations of (19) with respect to the coupling variables $\boldsymbol{u}^*_c = \left(\bar{\lambda}^*_{c,N+1/2} \quad \bar{\lambda}^*_{c,N+1}\right)^T \in \mathbb{R}^2$, i.e.

$$\boldsymbol{J}_{c\lambda} = \frac{\partial \bar{g}_{c\lambda}}{\partial \boldsymbol{u}^*_c}, \quad \boldsymbol{J}_{c\lambda,D} = \frac{\partial \bar{g}_{c\lambda,D}}{\partial \boldsymbol{u}^*_c}, \quad \boldsymbol{J}_{c\lambda,I} = \frac{\partial \bar{g}_{c\lambda,I}}{\partial \boldsymbol{u}^*_c}. \tag{20}$$

Making use of the partial derivatives, we can calculate the corrected coupling variables so that for D-Extension the coupling conditions $\bar{g}_{c\lambda}$ and $\bar{g}_{c\lambda,D}$ ($\bar{g}_{c\lambda}$ and $\bar{g}_{c\lambda,I}$ for I-Extension) are simultaneously fulfilled at the macro-time point $\bar{T}_{N+1}$. The linearized coupling equations are given by

$$\begin{aligned}
\bar{g}_{c\lambda} &:= \bar{g}^p_{c\lambda} + \boldsymbol{J}_{c\lambda} \cdot \begin{pmatrix} \bar{\lambda}_{c,N+1/2} - \bar{\lambda}^p_{c,N+1/2} \\ \bar{\lambda}_{c,N+1} - \bar{\lambda}^p_{c,N+1} \end{pmatrix} = 0, \\
\bar{g}_{c\lambda,D} &:= \bar{g}^p_{c\lambda,D} + \boldsymbol{J}_{c\lambda,D} \cdot \begin{pmatrix} \bar{\lambda}_{c,N+1/2} - \bar{\lambda}^p_{c,N+1/2} \\ \bar{\lambda}_{c,N+1} - \bar{\lambda}^p_{c,N+1} \end{pmatrix} = 0, \\
\bar{g}_{c\lambda,I} &:= \bar{g}^p_{c\lambda,I} + \boldsymbol{J}_{c\lambda,I} \cdot \begin{pmatrix} \bar{\lambda}_{c,N+1/2} - \bar{\lambda}^p_{c,N+1/2} \\ \bar{\lambda}_{c,N+1} - \bar{\lambda}^p_{c,N+1} \end{pmatrix} = 0.
\end{aligned} \tag{21}$$

Solving the corresponding linearized coupling equations gives the corrected coupling forces $\bar{\lambda}_{c,N+1/2}$ and $\bar{\lambda}_{c,N+1}$ for both the D-Extension and the I-Extension method.

Step 3: Corrector step

Applying an interpolation function with the corrected coupling forces $\bar{\lambda}_{c,N+1/2}$ and $\bar{\lambda}_{c,N+1}$ and substituting the coupling forces with the help of the coupling equations, an analytical integration yields the corrected state variables

$$\boldsymbol{z}_{N+1} = \boldsymbol{z}_{N+1}(\boldsymbol{z}_N, \boldsymbol{z}_{N-1}). \tag{22}$$

This system can symbolically be written as

$$\boldsymbol{A}_{N+1} \cdot \boldsymbol{z}_{N+1} + \boldsymbol{A}_N \cdot \boldsymbol{z}_N + \boldsymbol{A}_{N-1} \cdot \boldsymbol{z}_{N-1} = \boldsymbol{0}. \tag{23}$$

4 STABILITY ANALYSIS OF THE CO-SIMULATION METHODS

The numerical stability of a co-simulation method is defined by the spectral radius of the related system of recurrence equations. The spectral radius is – as outlined in Section 2 – a function of the 7 independent parameters defined in Eq. (3). Instead of using these parameters, it is more convenient to use the subsequent 7 independent parameters for representing the stability behavior

$$
\begin{aligned}
&\overline{\Lambda}_{r1} = -\frac{\bar{d}_1}{2}\,, \overline{\Lambda}_{i1} = \frac{1}{2}\sqrt{4\cdot\bar{c}_1 - \bar{d}_1^2}\,,\\
&\alpha_{m21} = \frac{m_2}{m_1}, \alpha_{\Lambda r21} = \frac{\overline{\Lambda}_{r2}}{\overline{\Lambda}_{r1}} = \frac{\alpha_{d21}}{\alpha_{m21}},\\
&\alpha_{\Lambda i21} = \frac{\overline{\Lambda}_{i2}}{\overline{\Lambda}_{i1}} = \frac{1}{\alpha_{m21}}\frac{\sqrt{4\alpha_{m21}\alpha_{c21}\bar{c}_1 - \alpha_{d21}^2\bar{d}_1^2}}{\sqrt{4\cdot\bar{c}_1 - \bar{d}_1^2}},\\
&\alpha_{\Lambda rc1} = \frac{\alpha_{dc1}}{\alpha_m^*}\,, \alpha_{\Lambda ic1} = \frac{1}{\alpha_m^*}\frac{\sqrt{4\alpha_m^*\alpha_{cc1}\bar{c}_1 - \alpha_{dc1}^2\bar{d}_1^2}}{\sqrt{4\cdot\bar{c}_1 - \bar{d}_1^2}} \quad \text{with} \quad \alpha_m^* = 2\frac{\alpha_{m21}}{1+\alpha_{m21}}.
\end{aligned}
\tag{24}
$$

By fixing 5 parameters, the spectral radius can be plotted as a function of the remaining 2 parameters. In accordance with the 2D stability plots for time integration schemes, where real and imaginary part of the eigenvalue of Dahlquist's test equation are used as axes, we present in the following 2D-stability plots for co-simulation methods, where the spectral radius is depicted as a function of $\overline{\Lambda}_{r1}$ and $\overline{\Lambda}_{i1}$. The five remaining parameters ($\alpha_{m21}, \alpha_{\Lambda r21}, \alpha_{\Lambda i21}, \alpha_{\Lambda rc1}$ and $\alpha_{\Lambda ic1}$) are assumed to be 1 (symmetrical test model) or 10 (unsymmetrical test model). It should be mentioned that the spectral radius has to be computed numerically. The solid circles in the plots indicate stable points, i.e. points for which $\rho < (1 + 10^{-10})$ holds. In order to reduce floating point errors, computation of ρ has been accomplished with 128 digits. Stability plots for the symmetrical and the unsymmetrical test model based on a force/force-decomposition approach can be found in Figure 6 and Figure 7 .

Compared with explicit co-simulation methods, implicit approaches exhibit a significant improvement of the stability behavior. Regarding implicit co-simulation algorithms, D-Extension methods show a better stability behavior than the direct methods. D-Extension in connection with quadratic approximation polynomials ($k = 2$) exhibits the best stability properties for both the symmetrical and the unsymmetrical test model. I-Extension shows for $k = 2$ also an improved stability behavior in comparison with the direct method.

To investigate the influence of the sub-step size on the stability properties, we consider again the I-Extension co-simulation approach for $k = 1$. Not using equidistant sampling points, the numerical stability may be improved. For the analysis, it is useful to define an additional parameter, namely $\alpha_T := (\bar{T}_{N+\alpha} - \bar{T}_N)/(\bar{T}_{N+1} - \bar{T}_N)$ with $\bar{T}_{N+\alpha} \in [\bar{T}_N,\ \bar{T}_{N+1}]$. Stability plots for different values of α_T for $k = 1$ are collected in Figure 8. As can be seen, the numerical stability can be improved for both the symmetrical and unsymmetrical model by modifying α_T.

5 CONCLUSION

Different coupling approaches, where the coupling is realized by constitutive laws, have been discussed within this manuscript. Making use of a linear two-mass oscillator, representing two coupled Dahlquist's equations, a detailed stability analysis has been carried out. Implicit algorithms have been investigated, which are based on a predictor-corrector approach. Also explicit methods have been considered, which only require one single integration step. Also, modified implicit methods have been analyzed, which make use of the derivatives (D-Extension) and integrals (I-Extension) of the constitutive equations. The extended methods

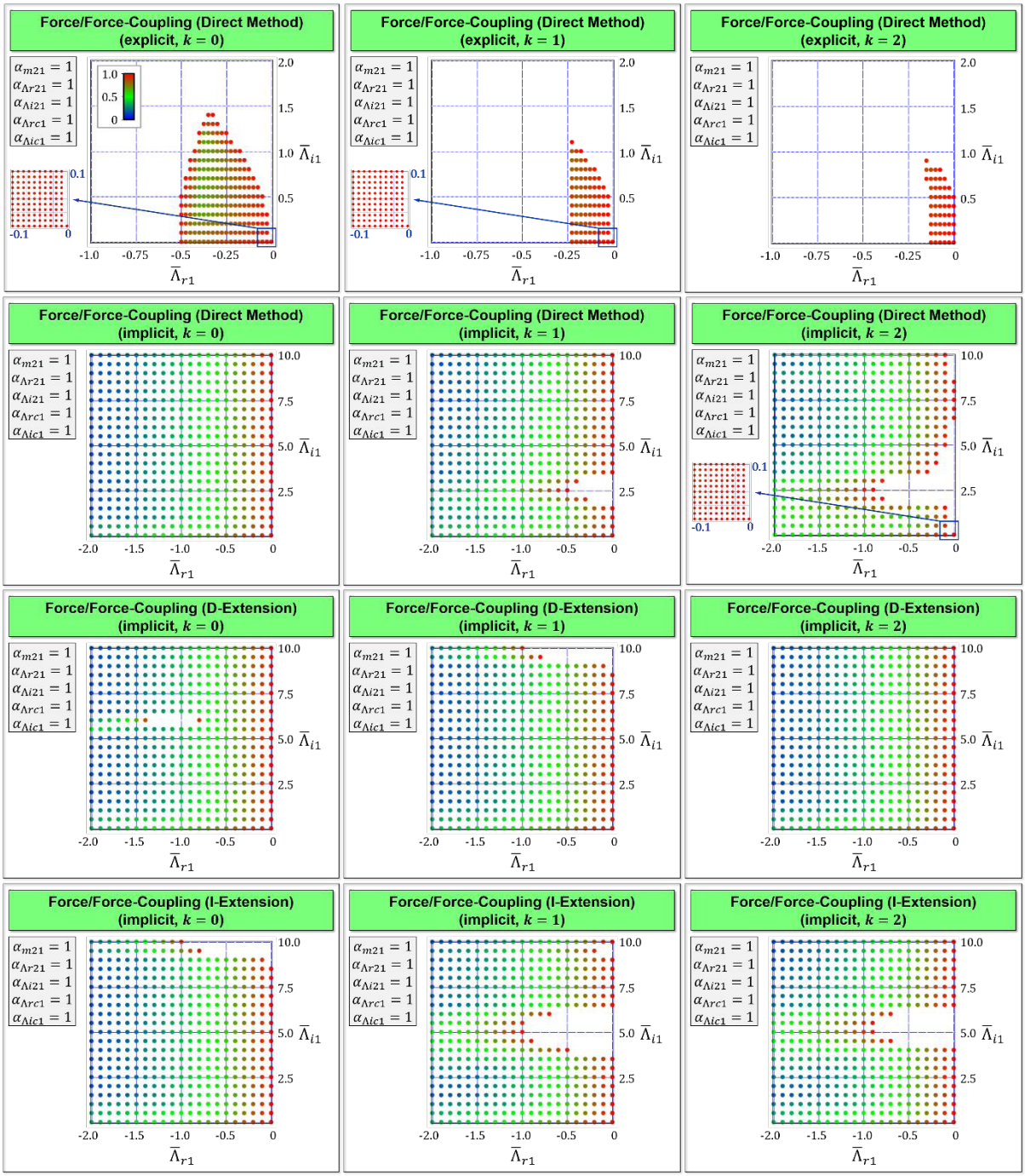

Figure 6: Stability plots for explicit and implicit co-simulation methods using force/force-decomposition with approximation order $k = 0,1,2$ for symmetrical test model

exhibit a better numerical stability behavior, especially in connection with higher-order approximation polynomials.

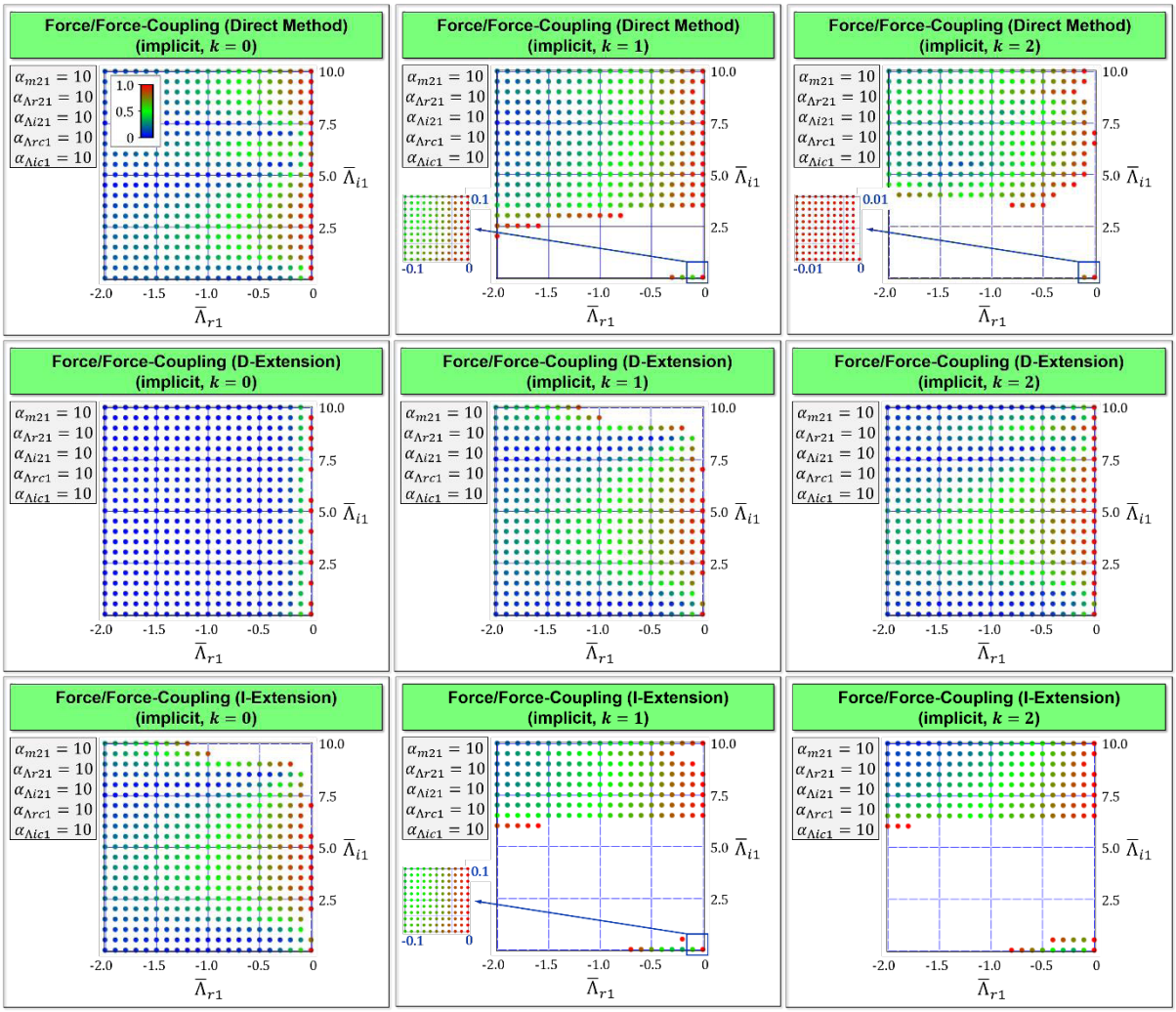

Figure 7: Stability plots for implicit co-simulation methods using force/force-decomposition with approximation order $k = 0,1,2$ for unsymmetrical test model

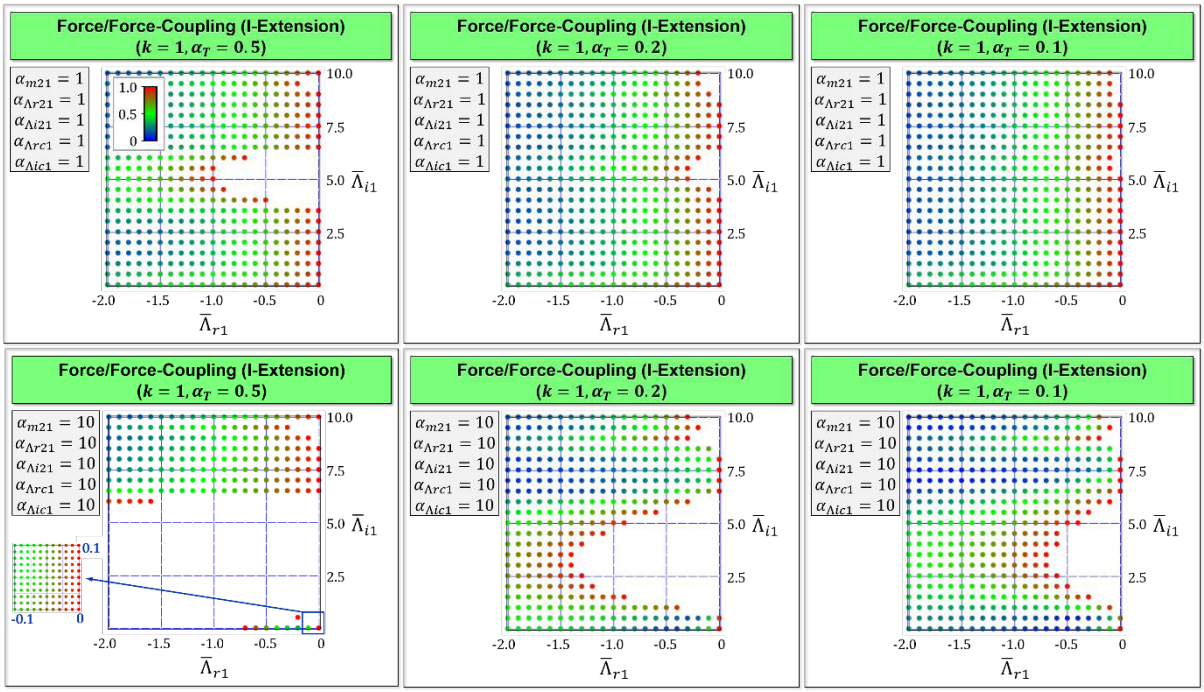

Figure 8: Stability plots for the I-Extension co-simulation method based on a force/force-decomposition approach with approximation order $k = 1$ for different values of α_T

REFERENCES

[1] Ambrósio, J., Pombo, J., Pereira, M., Antunes, P., and Mósca, A., A computational procedure for the dynamic analysis of the catenary-pantograph interaction in high-speed trains, *Journal of Theoretical and Applied Mechanics*, (2012) **50**: 681-699.

[2] Meynen, S., Mayer, J., and Schäfer, M., Coupling algorithms for the numerical simulation of fluid-structure-interaction problems, Proc. *ECCOMAS 2000: European Congress on Computational Methods in Applied Sciences and Engineering, Barcelona, Spain, Sept*, 11-14.

[3] Datar, M., Stanciulescu, I., and Negrut, D., A co-simulation environment for high-fidelity virtual prototyping of vehicle systems, *International Journal of Vehicle Systems Modelling and Testing*, (2012) **7**: 54-72.

[4] Daniel, W. J. T., A study of the stability of subcycling algorithms in structural dynamics, *Computer Methods in Applied Mechanics and Engineering*, (1998) **156**: 1-13.

[5] Schweizer, B., Li, P., and Lu, D., Explicit and Implicit Cosimulation Methods: Stability and Convergence Analysis for Different Solver Coupling Approaches, *Journal of Computational and Nonlinear Dynamics*, (2015) **10**: 051007-051012.

[6] Schweizer, B., Li, P., Lu, D., and Meyer, T., Stabilized implicit co-simulation methods: solver coupling based on constitutive laws, *Archive of Applied Mechanics*, (2015) **85**: 1559-1594.